Biochimica et Biophysica Acta (BBA) – Biomembranes Volume 1862, Issue 2, 1 February 2020, 183141: https://doi.org/10.1016/j.bbamem.2019.183141

Biophysical studies on the antimicrobial activity of linearized esculentin 2EM

Erum Malik[1], David A. Phoenix[2], Kamal Badiani[3], Timothy J Snape[4], Frederick Harris[1], Jaipaul Singh[1] Leslie Hugh Glyn Morton[1] and Sarah R. Dennison[4*]

[1]School of Forensic and Investigative Science, University of Central Lancashire Preston PR1 2HE, UK

[2]Office of the Vice Chancellor, London South Bank University, 103 Borough Road, London SE1 0AA, UK.

[3]Pepceuticals Limited, 4 Feldspar Close, Warrens Park, Enderby, Leicestershire, LE19 4JS, UK;

[4]School of Pharmacy and Biological Sciences, University of Central Lancashire, Preston PR1 2HE, UK

[*]To whom correspondence should be addressed Dr. S. R. Dennison.

Tel: +44 (0) 1772 894475

E-mail: srdennison1@uclan.ac.uk.

Key words: Linearized esculentin 2EM, α-helical structure, tilted peptide, Gram-positive bacteria, phosphatidylglycerol and cardiolipin.

Biochimica et Biophysica Acta (BBA) – Biomembranes Volume 1862, Issue 2, 1 February 2020, 183141: https://doi.org/10.1016/j.bbamem.2019.183141

ABSTRACT

Linearized esculentin 2 EM (E2EM-lin) from the frog, *Glandirana emeljanovi* was highly active against Gram-positive bacteria (minimum lethal concentration ≤ 5.0 μM) and strongly α-helical in the presence of lipid mimics of their membranes (> 55.0 %). The N-terminal α-helical structure adopted by E2EM-lin showed the potential to form a membrane interactive, tilted peptide with an hydrophobicity gradient over residues 9 to 23. E2EM-lin inserted strongly into lipid mimics of membranes from Gram-positive bacteria (maximal surface pressure changes ≥ 5.5 mN m^{-1}), inducing increased rigidity (Cs^{-1} ↑), thermodynamic instability ($\Delta G_{mix} < 0 \rightarrow \Delta G_{mix} > 0$) and high levels of lysis (> 50.0%). These effects appeared to be driven by the high anionic lipid content of membranes from Gram-positive bacteria; namely phosphatidylglycerol (PG) and cardiolipin (CL) species. The high levels of α-helicity (60.0%), interaction (maximal surface pressure change = 6.7 mN m^{-1}) and lysis (66.0%) shown by E2EM-lin with PG species was a major driver in the ability of the peptide to lyse and kill Gram-positive bacteria. E2EM-lin also showed high levels of α-helicity (62.0%) with CL species but only low levels of interaction (maximal surface pressure change = 2.9 mN m^{-1}) and lysis (21.0%) with the lipid. These combined data suggest that E2EM-lin has a specificity for killing Gram-positive bacteria that involves the formation of tilted structure and appears to be primarily driven by PG-mediated membranolysis. These structure / function relationships are used to help explain the pore forming process proposed to describe the membranolytic, antibacterial action of E2EM-lin.

Highlights

- E2EM-lin shows specificity and potent efficacy towards Gram-positive bacteria
- PG-driven membranolysis promotes E2EM-lin action against Gram-positive bacteria
- PE-driven membranolysis promotes E2EM-lin action against Gram-negative bacteria
- CL-mediated mechanisms contribute to E2EM-lin action against both bacterial types

1. INTRODUCTION

The occurrence of microorganisms with multiple drug resistance (MDR) coupled to the declining number of novel antimicrobial agents in the research pipeline is threatening a return to the pre-antibiotic era [1]. In response, the therapeutic development of antimicrobial peptides (AMPs) has been proposed as a potential solution to this problem [2] and the richest source of these peptides is the skin of amphibians [3, 4]. AMPs from frogs were the first to be commercially developed for clinical use [5], and currently, peptides from a wide variety of frogs, toads and salamanders are under investigation as therapeutically relevant antibacterial, antiviral, antifungal and antiprotozoan agents [3, 6]. In the search for novel AMPs, the true frogs, family Ranidae, has been a promising source as it is the most diverse and widely distributed group of anuran amphibians worldwide, occurring on all continents except Antarctica [7, 8]. The Ranidae have undergone many taxonomic reorganizations and phylogenetic studies [9-12], and currently, the online database, AmphibiaWeb, lists 22 genera with 407 species for this family [13]. There have also been attempts to derive a consistent nomenclature for AMPs of the Ranidae [9, 14, 15] and using the system proposed by Conlon (2008), these peptides are assigned to one of fourteen families on the basis of sequence similarity to prototypic peptides [9]. Major examples of these prototypic peptides include brevinin-1 and brevinin-2 [9], which were isolated from *Rana brevipoda porsa* [16], and esculentin-1 and esculentin-2 [9], which were identified in *Rana esculenta* [17]. The families of brevinins and esculentins are distributed across the genera of Ranidae [3, 18], ranging from Rana, which is the largest with over 100 species, to Glandirana, which is one of the newest and smallest with five species [13].

The archetypal species of the genus Glandirana is *Glandirana emeljanovi* [19], formerly known as *Rana rugosa*, which is distributed across northeastern China and the Korean peninsula [20]. It produces a suite of α-helical AMPs that were originally named gaegurins in reference to the Korean word for frog, Gaegury [21]. These peptides have been renamed since their discovery and several have been well characterised, including esculentin-2EM (gaegurin 4), brevinin-1EMa (gaegurin 5) and brevinin-1EMb (gaegurin 6) [19]. Along with their derivatives, these latter three AMPs have been shown to kill bacteria, fungi and protozoa [21-27], as well as possessing anticancer activity [22, 28, 29] and insulinotropic properties [30]. These AMPs and

their derivatives have also been investigated for potential therapeutic application; for example, brevinin-1Emb and its N-terminal homologue, PTP6, were highly effective against oral streptococci. These AMPs also acted synergistically with conventional oral antimicrobials, such as chlorhexidine, which led to the proposal that they might be suitable for development as agents for the prevention of dental caries [31]. There have been attempts to develop more efficient techniques for the production of esculentin-2EM (E2EM) and its derivatives as antimicrobials; for example, using *E. coli* as a host, recombinant E2EM, and recombinant hybrids of E2EM and the human AMP, LL-37, were efficiently generated and shown to have potent antibacterial activity [32, 33]. Another derivative of E2EM is the linear form of the peptide, E2EM-lin, which lacks the sole disulphide bond possessed by the parent peptide [19]. The primary focus of research on E2EM-lin appears to be investigation of the biological role of the C-terminal Rana box motif of E2EM [19, 34], a cysteine-stabilised, α-helical, loop-like fold that is conserved across many ranid AMPs [3, 4]. However, most recently, the membrane interactive form of E2EM-lin was shown to be highly thermostable in the presence of a range of bacterial membranes. It was suggested that the peptide, or its derivatives, might find application in the development of food packaging materials [35]. These packaging materials are formed from polymers which incorporate AMPs and are able to prolong the shelf life of the food product by inhibiting microbial growth on the surface of the product or the headspace inside the packaging [36, 37].

Despite its potential for commercial use, the mechanisms underpinning the antimicrobial activity of E2EM-lin are currently, not well characterised and have been investigated in the present study using a range of theoretical and biophysical techniques. These investigations showed that E2EM-lin has a potent, specificity for killing Gram-positive bacteria using a mode of action that appeared to be promoted by the high levels of anionic lipid in their membranes; namely, phosphatidylglycerol (PG) and cardiolipin (CL) species. The latter lipid promoted only low levels of membranolysis by E2EM-lin and potential roles for the lipid in the antibacterial mechanism of the peptide are being discussed. The primary driver in the mode of antibacterial action used by E2EM-lin appeared to be PG-mediated membranolysis, wherein the peptide's N-terminal region formed tilted structure to promote membrane pore formation. Based on our data, we propose a model for the PG-mediated antibacterial action of the peptide that also provides insight into both that of E2EM and that of a number of its truncated analogues.

2. MATERIALS AND METHODS

2.1 Materials

E2EM-lin (GILDTLKQFAKGVGKDLVKGAAQGVLSTVSCKLAKTC) was supplied by Pepceuticals (UK), synthesised by solid state synthesis and purified by HPLC to purity greater than 99%, confirmed by MALDI-TOF mass spectrometry (Supplementary Figure 1). Sodium phosphate monobasic, sodium diphosphate dibasic, sodium chloride, Sephadex G75, HEPES (4-(2-hydroxyethyl)-1-piperazineethanesulfonic acid) and EDTA (Ethylenediaminetetraacetic acid) were supplied by Sigma-Aldrich Ltd (UK). Nutrient agar, Nutrient Broth, Triton X-100 and ¼ strength Ringer solution tablets were supplied by Thermo Fisher Scientific (UK). Dimyristoyl phosphatidylglycerol (DMPG), dimyristoyl phosphatidylethanolamine (DMPE) and cardiolipin (CL) were supplied by Avanti Polar Lipids, Inc (Alabaster, AL). Calcein was supplied by Alfa Aesar and Milli Q water with a specific resistance of 18 Ω cm^{-1} was used for preparation of all stock solutions and buffers.

2.2 Methods

2.2.1 Theoretical analysis of E2EM-lin

The potential of E2EM-lin to form amphiphilic α-helical structure was investigated using the graphics function of Heliquest software (available online at http://heliquest.ipmc.cnrs.fr/ [38]) which represented the peptide as a two-dimensional axial projection taken perpendicular to the α-helical long axis and assuming an amino acid periodicity of 100° [39]. The potential of E2EM-lin segments to form tilted structures was determined according to extended hydrophobic moment methodology [40]. Tilted structures are α-helical segments that are characterized by an asymmetric distribution of hydrophobicity, or hydrophobicity gradient, along the α-helical long axis that causes the parent AMPs to penetrate membranes at a shallow angle of between 20° and 80°, thereby promoting a range of membrane destabilizing effects [41, 42]. Extended hydrophobic moment methodology determines the potential of AMPs to form tilted structure using sequence information alone and essentially, computes the mean hydrophobic moment, $< \mu H >$, and the mean hydrophobicity, $< H >$, of segments using the normalised consensus hydrophobicity scale of Eisenberg *et al.,* (1982) and a moving window of 11 residues [39]. These values of $< \mu H >$ and $< H >$ are then represented as data points on

the extended hydrophobic moment plot diagram, which identifies candidate tilted α-helix forming segments by the occurrence of their data points in the shaded area delineated on the extended plot diagram [40]. The potential of E2EM-lin to form a hydrophobicity gradient was investigated by amphiphilic profiling using -< μH > with a moving window of seven residues and the normalized consensus hydrophobicity scale of Eisenberg *et al.*, [42]. Essentially, this methodology uses sequence information alone to provide a visual representation of the hydrophobicity gradients associated with tilted structure that informs on their relative magnitude and direction along the α-helical long axis of the parent tilted structure [41, 42].

2.2.2 The preparation of bacterial cultures

Cell suspensions of the Gram-positive and Gram-negative test organisms (Table 1), were prepared as follows: Freeze – dried cultures grown on Nutrient agar were used to inoculate a series of 9 ml of sterile Nutrient broths in universal bottles . These samples were then incubated in an orbital shaker at 100 rpm and 37 ºC until reaching their exponential log phase, as determined by optical density (OD) measurements in the range 0.01 to 0.03 at λ = 600 nm. Each bacterial suspension was centrifuged at 15000 × *g* for 15 minutes at 21 ºC using a bench top centrifuge (ALC PK 120R) to form a cell pellet. The resulting cell pellets were resuspended in 9 ml Ringer's solution and centrifuged again, and the resulting pellets were resuspended in Ringer's solution to give a starting inoculum density of *circa* 5.8×10^8 CFU / ml.

2.2.3 The antibacterial properties of E2EM-lin

In order to evaluate the toxicity of E2EM-lin to bacterial cells, stock peptide in 25% Ringer's solution (150 μM), was diluted to give concentrations in the range 0.06 μM to 150 μM. Aliquots (500 μl) of the peptide at each concentration in this range were then inoculated with an equal amount of bacterial suspension (10 μl) and left to incubate for 12 hours at 37 °C. As a control, this procedure was repeated without the inclusion of E2EM-lin After incubation, each sample of was spread onto a Nutrient agar plate and incubated for 12 hours to determine the minimum peptide concentration that yielded no bacterial growth. Where no bacterial growth was observed, 10 μl samples of these E2EM – bacteria mixtures were used to inoculate 9.9 ml of fresh Nutrient broth and incubated for a further 12 hours. After incubation, these peptide - bacterial mixtures were spread onto Nutrient agar plates and where no bacterial growth had

occurred, the levels of E2EM-ln in that sample was taken as its minimum lethal concentration (MLC) for the bacterial strain concerned. These experiments were performed in quintuplicate and the mean value derived.

2.3.4 The preparation of total lipid extract from bacterial membranes

Cultures were prepared from *Bacillus subtilis*, *Staphylococcus aureus*, *Escherichia coli* and *Pseudomonas aeruginosa*, as described above, and in each case, total membrane lipid extracts were obtained from these cultures using a modified form of the methodology presented by Bligh and Dyer [43]. Essentially, for each bacterium, 9 ml aliquots of culture were taken and centrifuged at 15000 × *g* for 15 minutes at 21 ºC using a bench top centrifuge (ALC PK 120R) to form a cell pellet. These pellets were washed twice with ¼ strength Ringer solution and centrifuged at 15000 × g for 10 minutes. Each pellet was then resuspended in 100 µl of ¼ strength Ringer solution and the whole vortexed with 125 µl of a chloroform:methanol mixture (1:2, v/v) for 5 minutes. The resulting suspensions were then vortexed with 125 µl of chloroform for 5 minutes before 125 µl of water was added and the whole centrifuged at 600 × *g* for 5 minutes to obtain a two-phase system. The bottom, organic phase was then taken and concentrated by removing the solvent with N_2 gas before storage at -20 ºC.

2.3.5 The lysis of model membranes by E2EM-lin

To investigate the membranolytic ability of E2EM-lin, chloroformic solutions were prepared, which contained either the individual lipids, DMPG, CL or DMPE; lipid mixtures formed from DMPE and DMPG at ratios of 1:10, 1:20, 1:30, 1:50 and 1:100; lipid mimics of membranes from *E. coli*, *P. aeruginosa*, *B. subtilis* and *S. aureus* (Table 2); or lipid extracts from the membranes of each of these bacteria, prepared as described above. These chloroformic lipid solutions were then used to form small unilamellar vesicles (SUVs) and were dried under an N_2 (gas) stream before being placed under vacuum overnight. The resulting thin lipid films were hydrated using 5.0 mM HEPES, which contained 70 mM calcein, and these suspensions were then vortexed before being sonicated for 30 minutes and freeze-thawed 5 times. Untrapped calcein was separated from dye filled SUVs by gel filtration using a Sephadex G75 column, which was rehydrated overnight in 20 mM HEPES, 150 mM NaCl and 1.0 mM EDTA. The column was eluted with 5 mM HEPES pH 7.5 to produce solutions of SUVs with calcein entrapped. The rate of calcein leakage induced by E2EM-lin from these SUVs was then

determined as a function of peptide concentration. Stock solutions of E2EM-lin (90 µl) with concentrations in the range, 0 µM to 200 µM, were mixed with 30µl of calcein entrapped SUVs solutions and these samples made up to 3 ml with PBS, pH 7.4. The samples were left to incubate and after one hour, calcein fluorescence was measured using an FP-6500 spectrofluorometer (JASCO, UK) with an excitation wavelength of 490 nm and an emission wavelength of 520 nm. The % calcein leakage from SUVs was then calculated according to equation 1:

$$\%\ \text{dye release} = (([F_{Peptide}] - [F_{PBS}]) / ([F_{Triton}] - [F_{PBS}])) \times 100 \quad \ldots\ldots\ldots\ldots\ldots\ldots \text{Equation (1)}$$

where the fluorescence of calcein release by the peptide at 520 nm is denoted by $[F_{Peptide}]$, that released by PBS as $[F_{PBS}]$ and that released by Triton X-100 as $[F_{Triton}]$. In all cases, values of the % calcein released were determined in quintuplicate and the mean value derived.

2.3.6 The conformational behaviour of E2EM-lin

To investigate the conformational behaviour of E2EM-lin in aqueous solution and membrane mimicking solvents, the peptide was solubilised in either PBS (10 mM, pH 7.4), TFE and a 50 % (v/v) mixture of TFE / PBS (10 mM, pH 7.4) to give a final peptide concentration of 2.6 µM. The conformational behaviour of E2EM-lin in the presence of a range of SUVs was investigated by solubilising the peptide (final concentration of 0.1 mg ml^{-1}) in these SUVs at a lipid to peptide ratio of 1:100. SUVs were formed from either the individual lipids, DMPG, CL or DMPE; lipid mixtures formed from DMPE and DMPG at ratios of 1:10, 1:20, 1:30, 1:50 and 1:100; lipid mimics of membranes from *E. coli*, *P. aeruginosa*, *B. subtilis* and *S. aureus* (Table 2); or lipid extracts from the membranes of each of these bacteria, prepared as described above. In each case, these single lipids, lipid extracts, and lipid mixtures were dissolved separately in chloroform and dried under N_2 gas before being placed under vacuum for 4 hours. The resulting lipid films were rehydrated using PBS (10 mM, pH 7.40) sonicated for an hour or until the solution was no longer turbid, and then subjected to 5 cycles of freeze-thawing. Conformational analyses were conducted using a J-815 CD spectropolarimeter (Jasco, UK) at 20 °C, all as previously described [44]. Essentially, samples were placed in a quartz cell with a 10 mm path-length and four scans per sample were performed over a wavelength range of 260 to 180 nm at 0.5 nm intervals, using a band width of 2 nm and a scan speed 50 nm min^{-1}. All spectra were baseline corrected and the % α-helical content determined using the CDSSTR

method (protein reference set 3) from the DichroWeb server [45-47]. These experiments were repeated in quintuplicate and the levels of α- helicity obtained were averaged.

2.3.7 The surface activity of E2EM-lin

The surface activity of E2EM-lin was investigated using a 15 cm^2 Teflon Langmuir trough, wherein the peptide was injected into a PBS subphase (10 mM, pH 7.4) using a Hamilton micro syringe to give final peptide concentrations ranging from 0 to 2 μM. The resulting surface pressure changes were monitored and were plotted as a function of peptide concentration.

2.3.8 The lipid monolayer interactions of E2EM-lin

Monolayer experiments were performed using a 601M Langmuir trough (Biolin Scientific KSV NIMA, UK) equipped with moveable barriers. Surface pressure changes were monitored using a Whatman CH1 Whilemly paper plate attached to a microbalance [48, 49]. In all experiments the subphase of the Langmuir trough consisted of PBS buffer (10 mM, pH 7.4) prepared with Milli-Q-water (resistivity ≈ 18 MΩ cm) at 21± 1 °C.

2.3.8.1 Constant area analysis

The ability of E2EM-lin to interact with lipid monolayers was studied at constant area [48, 49]. Monolayers were formed by separately spreading chloroformic solutions onto a PBS subphase (10 mM, pH 7.4), which contained either the individual lipids DMPG, CL, or DMPE (0.5 mM); or lipid mixtures mimetic of membranes from *E. coli*, *P. aeruginosa*, *B. subtilis* and *S. aureus* (Table 2). After spreading these monolayers, solvent was allowed to evaporate for 30 minutes and then the barriers Langmuir trough were closed at a rate of 10 cm^2 min^{-1} to achieve a surface pressure of 30 mN m^{-1}. This surface pressure is generally taken to represent the packing density of naturally occurring cell membranes and was maintained throughout these experiments [50]. Monolayers were allowed to equilibrate for 10 minutes and E2EM-lin was injected into the subphase to give a final peptide concentration of 0.5 μM. The resulting changes in monolayer pressure were monitored and plotted as a function of time. Each experiment was repeated in quintuplicate.

2.3.8.2 Compression isotherm analysis

Compression isotherms were generated by spreading chloroformic solutions of lipid (1.0×10^{15} molecules) onto a PBS subphase (10 mM, pH 7.4), which contained either the individual lipids DMPG, CL, or DMPE (0.5 mM); or lipid mixtures mimetic of membranes from *E. coli*, *P. aeruginosa*, *B. subtilis* and *S. aureus* (Table 2). The solvent was allowed to evaporate for 10 minutes and the monolayer was allowed to settle for a further 20 minutes before the trough barriers were closed at a rate of 10 cm^2 per minute until monolayer collapse pressure was achieved. Surface pressure changes were monitored and plotted as a function of the area per lipid molecule. Corresponding experiments were then performed except that E2EM-lin was introduced into the PBS subphase (10 mM, pH 7.4) using a Hamilton syringe to give a final peptide concentration of 2 μM. All experiments were repeated in quintuplicate.

Thermodynamic analysis of lipid and lipid / peptide isotherms was undertaken and compressibility moduli were determined for these isotherms according to equation 4 [51]:

$$C_s^{-1} = -A\left(\frac{\delta\pi}{\delta A}\right) \quad \text{.....Equation (2).}$$

where π is the monolayer surface pressure and *A* represents area per peptide or lipid molecule in the monolayer.

The thermodynamic stability of these isotherms was also investigated by determining their Gibbs free energy of mixing (ΔG_{mix}) according to equation 5:

$$\Delta G_{mix} = \int [A_{1,2,3} - (X_1 A_1 + X_2 A_2 + X_3 A_3) d\pi \quad \text{.....Equation (3).}$$

where $A_{1,2,3}$ is the molecular area occupied by the mixed monolayer, A_1 - A_3 are the area per lipid molecule in the individual monolayers of component 1, 2, and 3, X_1, X_2, X_3 are the molar fractions of the components. Numerical data were calculated from these compression isotherms

according to the mathematical method of Simpson [52]. ΔG_{mix} is used to measure the relative stability of monolayers associated with the miscibility energetics of their individual lipid components where thermodynamically stable and unstable monolayers are indicated by negative and positive values of ΔG_{mix} respectively [50].

2.3.9 Statistical analysis

Unless otherwise stated, the results are presented as mean values ± standard errors (SE) of the mean. Initially, the normal distribution of the data was analysed by Skewness Kurtosis tests. Significant differences between mean values were further analysed by using a one-way ANOVA test, based on a null hypothesis that there is no significant difference between the mean values.

3. RESULTS

3.1 The theoretical analysis and surface activity of E2EM-lin

Confirming previous suggestions [19], when modelled as a two-dimensional axial projection, the entire E2EM-lin sequence only showed the potential to form an α-helix with ill-defined amphiphilicity (Figure 1A). However, sequences defined by residues 1-23 (E2EM-lin (1-23), Figure 1B) and residues 25-37 (E2EM-lin (25-37), Figure 1C) showed the potential to form two strongly amphiphilic α-helices. These α-helices exhibited hydrophobic arc sizes of 200^{o} and 120^{o} respectively and were linked by the intervening glycine residue, G24 (Figures 1B and 1C). Analysis of E2EM-lin (1-23) and E2EM-lin (25-37) using extended hydrophobic moment plot methodology yielded values of $< \mu H > = 0.43$ and $< H > = 0.06$, and $< \mu H > = 0.67$ and $< H > = 0.09$, respectively. When plotted on the extended plot diagram, the resulting data points lay within the shaded area of the diagram, predicting that both α-helices had the potential to form tilted peptides (Figure 2A), which are characterized by a hydrophobicity gradient along the α-helical long axis [42]. Amphiphilic profiling revealed that E2EM-lin possessed a hydrophobicity gradient, which increased in the N → C direction and stretched over residues 9 to 31, encompassing both E2EM-lin (1-23) and E2EM-lin (25-37) (Figure 2B).

Biochimica et Biophysica Acta (BBA) – Biomembranes Volume 1862, Issue 2, 1 February 2020, 183141: https://doi.org/10.1016/j.bbamem.2019.183141

Figure 1. Helical wheel analysis of E2EM-lin

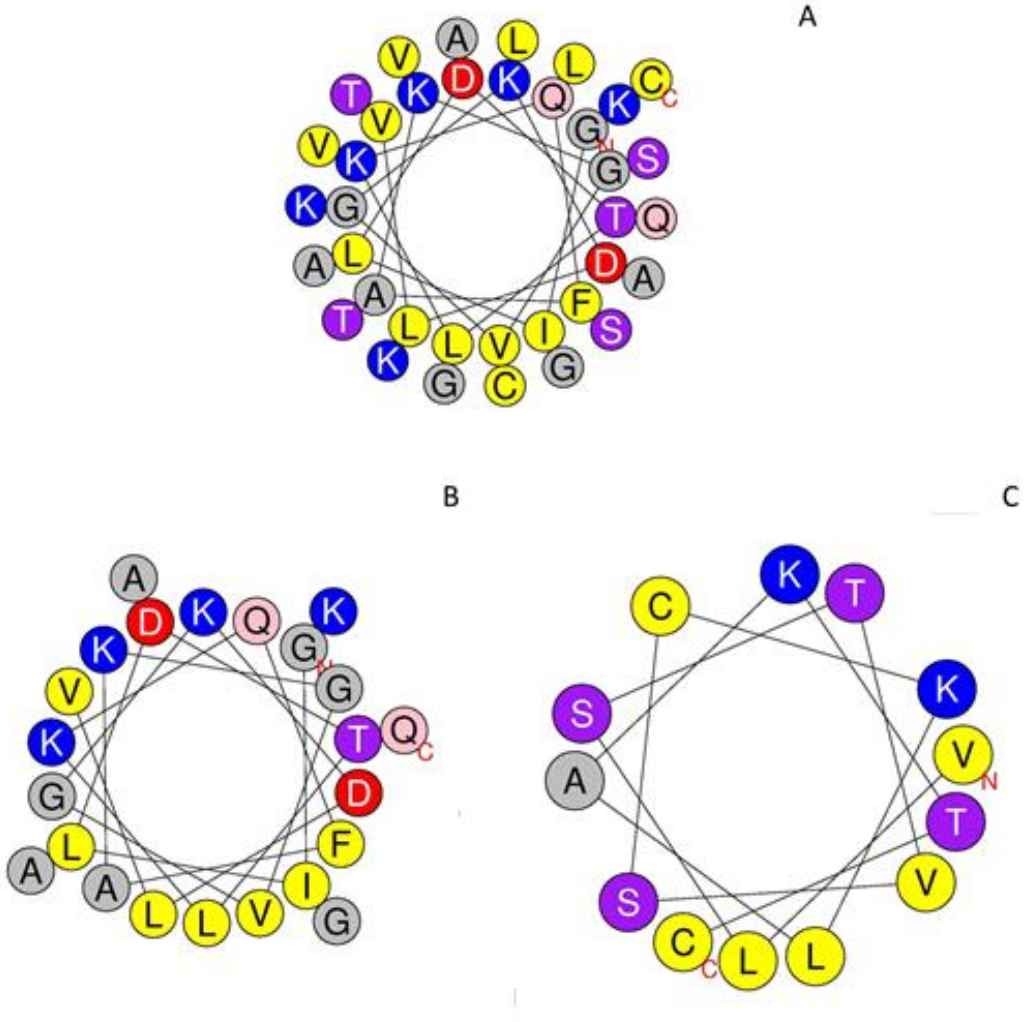

Figure 1 shows E2EM-lin modelled as two dimensional axial projections [38]. Figure 1A shows that in an α-helical conformation, the entire sequence of the peptide (GILDTLKQFAKGVGKDLVKGAAQGVLSTVSCKLAKTC) possesses only ill-defined amphiphilicity with no clear segregation between polar and non-polar residues. Figures 1B and 1C show that the peptide could potentially form two strongly amphiphilic α-helices that are linked by the intervening glycine residue (G24), as previously shown [19]. The first of these α-helices is defined by residues 1-23 and exhibits a hydrophobic face with an arc size of 200^{o}, along with a hydrophilic face that has a net cationic charge due to the presence of multiple lysine and aspartic acid residues (Figure 1B). The second of these α-helices is defined by residues 25-37 and possesses a hydrophobic face with an arc size 120^{o}, complemented by a hydrophilic face formed from polar and lysine residues (Figure 1C).

Figure 2. The potential of E2EM-lin to form tilted structure

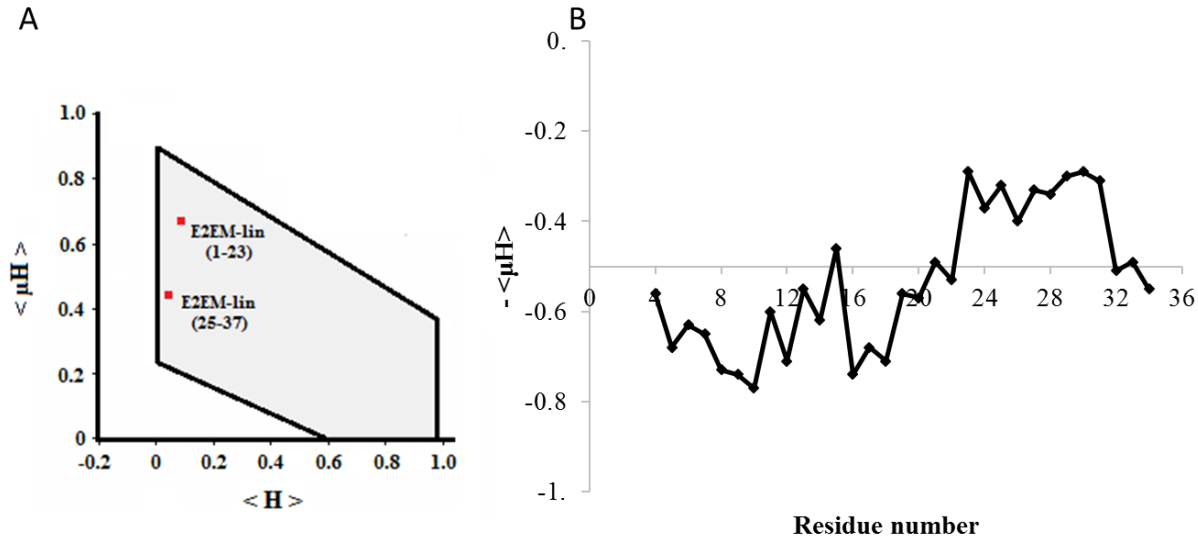

Figure 2 shows theoretical analyses of the E2EM-lin α-helices potential for tilted peptide formation. In Figure 2A, extended hydrophobic moment plot methodology shows that the data points representing E2EM-lin (1-23) and E2EM-lin (25-37) [< μH > = 0.43 and < H > = 0.06, and < μH > = 0.67 and < H > = 0.09, respectively] lie in the shaded area of the plot diagram. This location indicates the potential to form tilted peptides, which are characterized by a hydrophobicity gradient along the α-helical long axis [42]. In Figure 2B, amphiphilic profiling shows that E2EM-lin possesses a hydrophobicity gradient, which increases in the N → C direction and stretches over residues 9 to 31, encompassing both E2EM-lin (1-23) and E2EM-lin (25-37). This asymmetric distribution of hydrophobicity causes the tilted structure of AMPs to penetrate membranes at a shallow angle of between 20° and 80°, thereby promoting a range of membrane destabilizing effects [41, 42].

3.2 The antibacterial properties and membranolytic ability of E2EM-lin

Assay of E2EM-lin against a panel of bacteria showed that the peptide had weak activity against Gram-negative organisms, with MLCs that were ≥ 75.0 μM. but possessed potent efficacy towards Gram-positive bacteria, with MLCs that were ≤ 6.5 μM (Table 1). This was confirmed by statistical analysis which showed that there was a significant difference between the MLCs of E2EM-lin for Gram-negative and Gram-positive bacteria [$F_{2,21}$ = 33.61; p = 0.00]. These observations indicated that E2EM-lin has a strong preference for Gram-positive bacteria, which is consistent with data reported by previous authors [19, 53], and to investigate this preference further, *S. aureus* and *B. subtilis* were taken as representative Gram-positive organisms, whilst *E. coli* and *P. aeruginosa*, were chosen to represent Gram-negative bacteria. Consistent with a preference for Gram-positive bacteria, calcein release assay showed

that E2EM-lin lysed mimics of *S. aureus* and *B. subtilis* membranes (> 58.0%, Table 2) more strongly than those of *E. coli* and *P. aeruginosa* membranes (≤ 45.0%, Table 2). These data clearly suggested that the peptide has a greater lytic efficacy against membranes from Gram-positive bacteria in comparison to those from Gram-negative bacteria, which was confirmed by statistical analysis [$F_{3, 11} = 67.0$; $p = 0.00$]. The correlation of these lysis levels (Table 2) with the MLCs of the peptide against the corresponding organisms (Table 1) clearly suggested that the E2EM-lin killed bacteria *via* membranolytic mechanisms. Moreover, this correlation also suggested that the preference of the peptide for Gram-positive organisms was related to differences in the membrane compositions of these two bacterial classes. Membranes from *B. subtilis* and *S. aureus* are predominantly formed from CL and PG lipids, whereas those from *E. coli* and *P. aeruginosa* are primarily composed of phosphatidylethanolamine (PE) lipids (Table 2). Consistent with this observation, E2EM-lin induced levels of lysis that were 66.0% in the case SUVs formed from DMPG (Table 2) and were reduced as DMPE was introduced into the composition of these SUVs, reaching 41.0% for SUVs formed solely from DMPE (Table 2). However, the peptide showed a varying ability to interact with anionic SUVs, inducing only low levels of lysis with those formed from CL (20.0%, Table 2), and statistical analysis indicated that there was a significant difference between the levels of lysis induced by E2EM-lin with SUVs formed from either DMPG, DMPE or CL [$F_{4, 14} = 10$; $p = 0.001$]. Hence, these results clearly suggested that CL does not directly promote the membranolytic activity of E2EM-lin and would seem to exclude the peptide from AMPs that target CL domains of bacterial membranes to promote this mode of antibacterial activity [54-57].

Table 1. The antibacterial activity of E2EM-lin.

Bacteria and NCIMB strain number	MLCs of E2EM-lin (μM)
Gram-positive organisms	
Micrococcus luteus (196)	3.13
Streptococcus mutans (11723)	3.13
Streptococcus pyogenes (11841)	6.25
Staphylococcus aureus (1671)	3.13
Staphylococcus epidermis (8558)	3.13
Bacillus subtilis (8054)	6.25
Gram-negative organisms	
Klebsiella pneumoniae (13438)	100.0
Klebsiella aerogenes (10102)	200.0
Escherichia coli (887a)	100.0
Pseudomonas aeruginosa (8295)	75.0
Proteus mirabilis (13283)	200.0

In Table 1, MLCs are the minimum lethal concentrations of E2EM-lin required to kill bacteria, determined as described above, and the data are the mean of five replicates.

3.3 The conformational behaviour and membrane interactions of E2EM-lin

CD spectroscopy showed that in aqueous solution (PBS, 10.0 mM, pH 7.4), E2EM-lin possessed < 10.0 % α-helical structure and was predominantly formed from random coil and β-type structures (Supplementary Figure 2). However, the peptide was found to be strongly surface active at an air / water interface (Maximal surface pressure changes of 21 mNm^{-1}, Figure 6) and previous work has predicted that under these experimental conditions, E2EM-lin adopts an α-helical conformation [35]. The peptide adopted high levels of α-helicity that were > 65.0 % when solubilized in the membrane mimicking solvent, TFE, or a 50 % (v/v) mixture of TFE / PBS (10 mM, pH 7.4), (Supplementary Figure 2). E2EM-lin also showed the ability to adopt α-helical structure in the presence of SUVs mimetic of bacterial membranes, formed from either lipid mixtures or native bacterial lipids (40.2% to 61.0%) (Figure 3, Table 2). In

combination, these observations show that the peptide is generally active in an amphiphilic interfacial environment *via* the adoption of α-helical structure.

E2EM-lin adopted levels of α-helicity were higher for mimics of *S. aureus* and *B. subtilis* membranes (> 55.0%) than those of *E. coli* and *P. aeruginosa* membranes (< 45.0%) (Figure 3, Table 2). Statistical analysis confirmed that these differences in the α-helicity of E2EM-lin were significant in the case of both membranes formed from lipid mixtures [$F_{3, 11}$ = 7392.3; p = 0.00] and those formed from native bacterial lipids [$F_{3, 11}$ = 594.0; p = 0.00]. The rank order of α-helicity levels adopted by E2EM-lin in the presence of membrane mimics from *S. aureus*, *B. subtilis*, *E. coli* and *P. aeruginosa* membranes (Figure 3, Table 2) also correlated with that of the lytic ability shown by E2EM-lin for these organisms (Table 2). This correlation suggested that the higher levels of α-helicity induced in the peptide by the membranes of Gram-positive bacteria promoted the greater lytic activity shown by E2EM-lin for these membranes (Table 2). Strongly supporting this suggestion, E2EM-lin showed a greater ability to partition into monolayer mimics of membranes from *S. aureus* and *B. subtilis* (maximal surface pressure changes ≥ 5.9 mN m^{-1}, Figure 7B) as compared to those of *E. coli* and *P. aeruginosa* (maximal surface pressure changes ≤ 4.8 mN m^{-1}, Figure 7B). Moreover, the high levels of these surface pressure changes clearly indicated that the peptide was able to deeply penetrate the hydrophobic acyl chain region of these membrane mimics, consistent with membranolyic ability [50].

To further investigate the role of individual lipids in the preference of E2EM-lin for Gram-positive bacteria, the conformational and partitioning behaviour of the peptide with model membranes formed from either, DMPG, DMPE or CL was studied (Figure 4 and Figure 5). These studies showed that E2EM-lin possessed levels of α-helicity that were 60.0% in the presence of SUVs formed solely from DMPG and were reduced as DMPE was introduced into the composition of these SUVs, reaching 40.5% for SUVs formed solely from DMPE (Figure 4, Figure 5, Table 2). Statistical analysis showed there was a significant different between the levels of α-helicity observed in E2EM-lin across these peptide to lipid ratios [$F_{4, 14}$ = 75.6; p = 0.000]. The rank order of these α-helicity levels correlated strongly with that of the lytic ability shown by E2EM-lin towards SUVs with the corresponding DMPG / DMPE compositions (Table 2). In general, increasing the α-helicity of AMPs enlarges their hydrophilic and hydrophobic surfaces, thereby enhancing their capacity to penetrate and lyse membranes [2,

41]. In combination, these data strongly suggested that the induction of α-helical structure in E2EM-lin by PG plays a major role not only in promoting the membranolytic antibacterial action of the peptide but also its preference for killing Gram-positive bacteria. Consistent with this suggestion, E2EM-lin induced maximal surface pressure changes of 6.7 mN m^{-1} in monolayers formed from DMPG that were reduced to 4.2 mN m^{-1} in the case of those formed from DMPE (Figure 7A). The high levels of these surface pressure changes also indicated that the partitioning of the peptide into bacterial membranes involved strong contributions from electrostatic and hydrophobic forces [50]. These observations clearly reflected the strongly amphiphilic nature of the α-helical structure formed by E2EM-lin (Figure 1A and Figure 1B).

E2EM-lin induced maximal surface pressure changes of 2.9 mN m^{-1} in monolayers formed from CL (Figure 7A), which are levels of partitioning that indicate head group associations [50] and are consistent with the low ability of the peptide to lyse SUVs formed from the lipid (Table 2). However, E2EM-lin adopted levels of α-helical structure in the presence of SUVs formed from CL that were 62% and very close to the levels of α-helicity adopted by the peptide in the case of SUVs formed from DMPG (Figure 4, Table 2). These data clearly showed that although CL induced conformational changes in E2EM-lin that were similar to those induced by DMPG, in comparison, they promoted greatly diminished levels of membrane interaction (Figure 7A, Table 2). In combination, these observations suggest that CL is able to promote electrostatic binding to the membrane by E2EM-lin and stabilization of the peptide's α-helical structure, but not the levels of partitioning required for membranolysis and antibacterial activity. It would seem that some property of the lipid inhibits or reduces the ability of E2EM-lin to partition into membranes and similar effects have been reported for other AMPs. In these cases, CL-mediated changes to the structural properties of membranes prevented the induction of membranolysis by these peptides but not their surface binding [58-60]. However, there is also the possibility that CL can promote the antibacterial action of E2EM-lin by mechanisms where direct membrane lysis does not play a major role. Several recent studies on AMPs have suggested that the CL-mediated partitioning of these peptides into bacterial membranes promotes cell death through secondary effects induced by changes to the biophysical properties of these membranes [61, 62].

Table 2. The levels of α-helicity and lysis shown by E2EM-lin with lipid SUVs.

Composition of SUVs formed from lipids and lipid mimics of bacterial membranes	**Membrane lysis (%)**	**α-helicity of E2EM-lin (%)**
CL	20.0	62.0
DMPG	66.0	60.0
DMPE:DMPG ratio 1:100	64.5	60.0
DMPE:DMPG ratio 1:50	56.6	58.0
DMPE:DMPG ratio 1:30	52.5	54.0
DMPE:DMPG ratio 1:20	48.0	50.0
DMPE:DMPG ratio 1:10	44.0	46.0
DMPE	41.0	40.5
B. subtilis: DMPE:DMPG:CL molar ratio 10:29:47	60.0	60.3
B. subtilis: lipid extracts of membranes	58.0	60.5
S. aureus: DMPG:CL molar ratio 57:43	57.0	58.0
S. aureus: lipid extracts of membranes	53.0	56.3
E. coli: DMPE:DMPG:CL molar ratio 82:6:12	45.0	40.2
E. coli: lipid extracts of membranes	41.0	40.3
P. aeruginosa: DMPE:DMPG:CL molar ratio 68:19:11	37.0	42.0
P. aeruginosa: lipid extracts of membranes	33.0	41.8

In Table 2, DMPG = dimyristoyl phosphatidylglycerol, DMPE = dimyristoyl phosphatidylethanolamine and CL = cardiolipin. Data for the lipid composition of bacterial membranes was taken from [63, 64].

Figure 3. CD analysis of E2EM-lin in the presence of model bacterial membranes

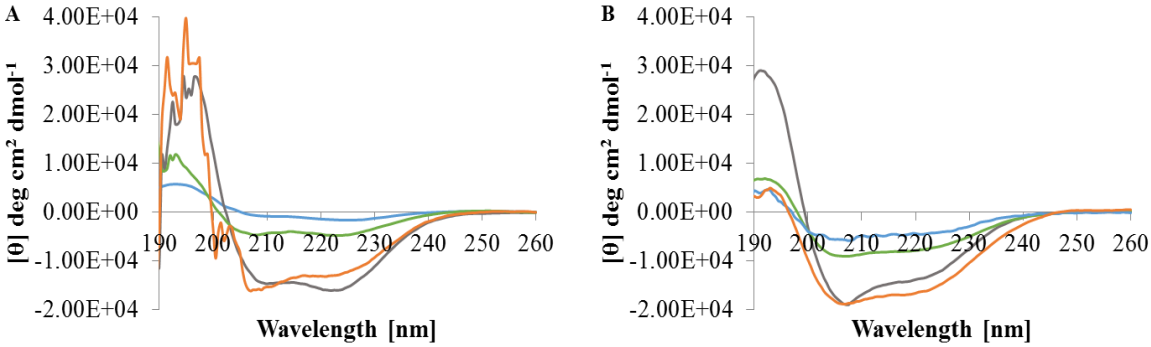

Figure 3 shows CD spectra for E2EM-lin in the presence of model bacterial membranes. In all cases, these spectra show typical α-helical structure for E2EM-lin with two minima near the 230 to 210 nm region and maxima near 195 nm [44]. In Figure 3A, curves are shown for the structure of E2EM-lin in the presence of lipid mixtures (Table 1) representing membranes of *E. coli* (Blue), *P. aeruginosa* (Green), *S. aureus* (Orange) and *B. subtilis* (Grey). In Figure 3B, curves are shown for the structure of E2EM-lin in the presence of native bacterial lipids representing membranes *E. coli* (Blue), *P. aeruginosa* (Green), *S. aureus* (Orange) and *B. subtilis* (Grey). Analysis of these spectra showed that E2EM-lin adopted high levels of α-helical structure in the presence of bacterial membranes (40.2% to 61.0%), which were, however, higher in the case of Gram-positive bacteria (58.0% to 61%) as compared to Gram-negative bacteria (40.2% to 42.0%) (Table 2).

Figure 4. CD analysis of E2EM-lin in the presence of individual lipid membranes

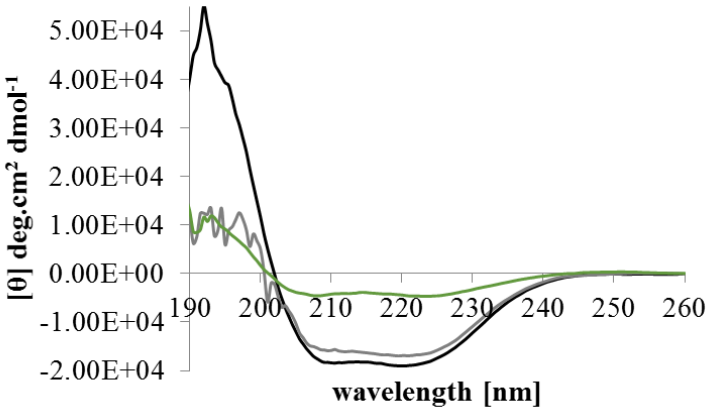

Figure 4 shows CD spectra for E2EM-lin in the presence of individual lipids at an L:P ratio of 100:1. In all cases, these curves possesses minima in the range 210 nm to 224 nm and a maximum at 193 nm, which is typical of α-helical structure [44]. Analysis of these spectra E2EM-lin was 60.0% in the case of DMPG (Black), 62.0% in that of CL (Grey) and 40.0% in that of DMPE (Green) (Table 2).

Figure 5. CD analysis of E2EM-lin in the presence of DMPE / DMPG membranes

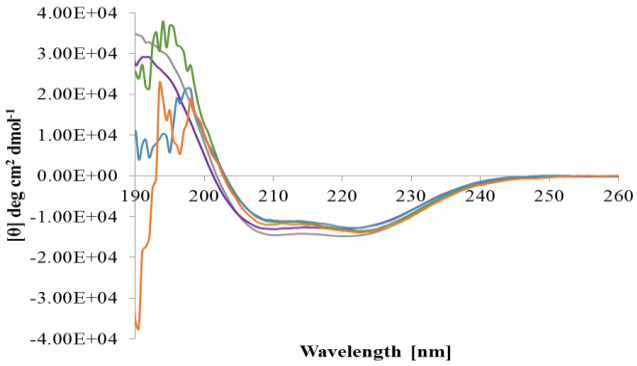

Figure 5 shows CD spectra for E2EM-lin in the presence of membranes formed from DMPE and DMPG where the lipid to peptide:ratio was maintained at 100:1 and the PE:PG ratio was varied between 1:10 and 1:100. In all cases, these curves possesses minima in the range 210 nm to 224 nm and a maxim around 193 nm, which is typical of α-helical structure [44]. Analysis of these spectra showed that E2EM-lin was 46.0% in the case of a DMPE: DMPG ratio of 1:10 (Orange), 50.0% in that of a 1:20 ratio (Green), 54.0% in that of a 1:30 ratio (Purple), 58.0% in that of 1:50 ratio (Blue) and 60.0% in that of a 1:100 ratio (Grey) (Table 2).

Figure 6. The surface activity of E2EM-lin

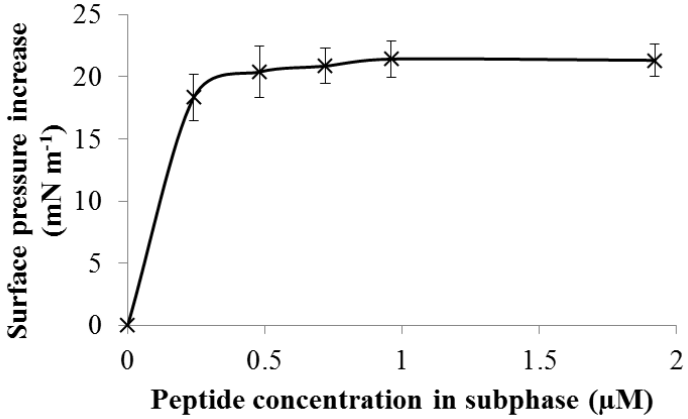

Figure 6 shows the surface activity of E2EM-lin at an air/water subphase. The peptide was introduced into the PBS subphase (10 mM, pH 7.4) of a 15 cm^2 Teflon Langmuir trough, and the resulting surface pressure changes plotted as a function of peptide concentration. Surface pressure changes induced by E2EM-lin increased rapidly up to a concentration of *circa* 0.5 μM when maximal surface pressure changes of 21 mNm^{-1} were observed. Above this peptide concentration, maximal surface pressure changes became independent of E2EM-lin levels,

indicating that the air / buffer interface was saturated with molecules of the peptide. These data indicate that E2EM-lin is highly surface active, and in each case, the data are the mean of five replicates and error bars are the standard error of the mean.

Figure 7. The interactions of E2EM-lin with lipid monolayers

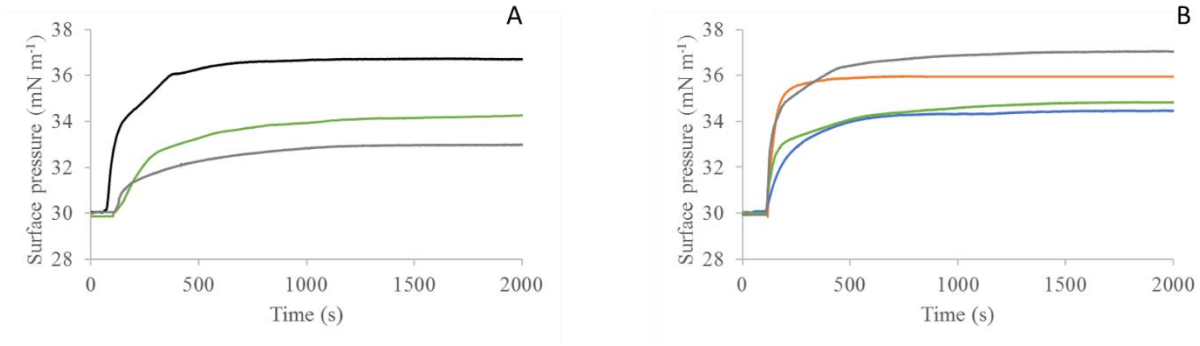

Figure 7 shows interactions of E2EM-lin with lipid monolayers. In Figure 7A, the peptide interacts with monolayers formed from DMPG (Black), CL (Grey) and DMPE (Green). The surface pressure increases induced by these interactions generally follow hyperbolic kinetics and show maximal values that are 6.7 mN m^{-1} in the case of DMPG, 2.9 mN m^{-1} in that of CL and 4.2 mN m^{-1} in that of DMPE. The levels of these surface pressure changes show that E2EM-lin has the general ability to partition strongly into anionic and zwitterionic lipid monolayers, indicating a role for both electrostatic interactions and hydrophobic forces. In Figure 7B, E2EM-lin interacts with monolayers formed from lipid mimics of membranes from *B. subtilis* (Grey), *S. aureus* (Orange), *E. coli* (Blue) and *P. aeruginosa* (Green). These interactions induce maximal surface pressure increases that were 7.1 mN m^{-1} in the case of *S. aureus*, 5.9 mN m^{-1} in that of *B. subtilis*, 4.5 mN m^{-1} in that of *E. coli* and 4.8 mN m^{-1} in that of *P. aeruginosa*. These data show that the peptide has the ability to partition into the membranes of both Gram-positive and Gram-negative bacteria, although this ability appears to be stronger in the case of the former organisms. In each case, the data are the mean of five replicates.

3.4 The thermodynamic analysis of E2EM-lin interactions with bacterial membranes

Langmuir-Blodgett troughs were used to generate compression isotherms for monolayers formed from either DMPG, CL or DMPE; or monolayer mimics of membranes of either *B. subtilis*, *S. aureus*, *E. coli*, or *P. aeruginosa*; all in the presence and absence of E2EM-lin (Supplementary Figure 3). Analysis of these isotherms showed that these mimics of bacterial membranes possessed C_s^{-1} values ranging from 19.02 mN m^{-1} to 29.27 mN m^{-1} in the absence of the peptide, indicating that they were in the liquid expanded phase and fluid at this compression pressure (Table 3) [50]. However, upon the addition of E2EM-lin to each of these lipid monolayer systems, C_s^{-1} increased, with values ranging from 35.69 mN m^{-1} to 49.03 mN

m^{-1} (Table 3). These data signified a general rise in the lateral pressure of monolayers and led to increases in their rigidity and lipid packing density, consistent with partitioning by the peptide [50]. Analysis of isotherms also generated values of ΔG_{mix} for monolayer mimics of membranes from *B. subtilis*, *S. aureus*, *E. coli*, or *P. aeruginosa*; all in the presence and absence of E2EM-lin (Supplementary Figure 3). In the absence of the peptide, these monolayer mimics of bacterial membranes were thermodynamically stable with values of $\Delta G_{mix} < 0$. In the presence of E2EM-lin, they became thermodynamically unstable with values of $\Delta G_{mix} > 0$ (Table 3), indicating that partitioning by the peptide had altered their lipid packing characteristics. Similar changes in ΔG_{mix} and C_s^{-1} (Table 3) have been reported for a number of AMPs that appear to use carpet type and tilted type mechanisms to promote their membranolytic, antibacterial action [65-67]. In combination, these observations support monolayer (Figure 7B) and lysis data (Table 3), reinforcing the suggestion that the amphiphilic and tilted characteristics of α-helical E2EM-lin play a major role in facilitating the membranolytic, antibacterial activity of the peptide. It is possible that these changes in ΔG_{mix} and C_s^{-1} (Table 3) also relate to CL-mediated interactions between E2EM-lin and bacterial membranes that promote non-membranolytic mechanisms of antibacterial action. Changes to membrane properties similar to those revealed by the thermodynamic analysis of E2EM-lin interactions with bacterial membrane mimics (Table 3) were demonstrated for the CL-mediated membrane partitioning of the non-membranolytic AMPs described above [61, 62]. For example, the insertion of these peptides, into the membranes of both Gram-positive and Gram-negative bacteria, promoted lipid reorganisation, changes to lipid packing characteristics and the perturbation of acyl chain order [61, 62].

Table 3. Thermodynamic analysis of E2EM-lin

Bacterial membranes	**C_s^{-1} (mN m^{-1})**		**ΔG_{mix} (kJ mol^{-1})**	
	- E2EM-lin	**+ E2EM-lin**	**- E2EM-lin**	**+ E2EM-lin**
B. subtilis	23.28	49.03	-26.38	51.60
S. aureus	19.02	47.13	-31.95	50.91
E. coli	29.27	36.22	-6.34	78.22
P. aeruginosa	19.32	35.69	-39.63	72.70

4. DISCUSSION

E2EM-lin displayed potent activity against Gram-positive bacteria at levels in the low micromolar range that are appropriate to therapeutic development [2] but showed only weak action towards Gram-negative organisms (Table 1). This pattern of antibacterial activity and efficacy is highly similar to that of E2EM [21, 25, 27, 33, 68], which clearly supports the view that the disulphide bond in the Rana box region of the latter peptide is not essential for action against prokaryotes [19]. Similar results have been recently reported for other amphibian AMPs [69] and it may be that the Rana box of E2EM serves other biological functions rather than playing a role in the peptide's antibacterial activity. For example, it has been shown that the presence of the disulphide bond in this motif is essential to the ability of brevinin-1EMb to stimulate insulin secretion in pancreatic β cells [30]..

E2EM-lin showed conformational behaviour (Figure 3, Table 2) and induced changes to the properties and integrity of membranes (Figure 7B, Table 2, Table 3) that are consistent with work proposing that the ability of the peptide to kill bacteria involves the permeabilization of their membranes. An experimentally supported, pore forming mechanism that is similar to that used by E2EM has been proposed to explain the process of membrane permeabilization by E2EM-lin. [19, 35, 70]. The present study has shown that the membrane interactions of E2EM-lin involve novel, unreported structure / function relationships that appear to help explain pore formation by E2EM-lin. In response, these structure / function relationships have been used to generate a more detailed model for the pore forming activity of E2EM-lin, which is depicted in Figure 8. In the early stages of this model, E2EM-lin is largely unstructured in aqueous solution, primarily formed from random coil and β-type structures (Supplementary Figure 2), and is strongly cationic (Figure 1), which facilitates the targeting of anionic components of the bacterial cell membrane (Figure 8A). Localization of the peptide to the anisotropic environment of the interface provided by these membranes promotes the adoption of α-helical structure (Figure 3, Table 2), which is strongly amphiphilic (Figure 1). Possession of this secondary architecture facilitates the partitioning of α-helical E2EM-lin into membranes *via*

electrostatic associations with the lipid head-group region and hydrophobic interactions with the acyl chain core of the membrane (Figure 8B).

Figure 8. A model for the membrane interactions of E2EM-lin

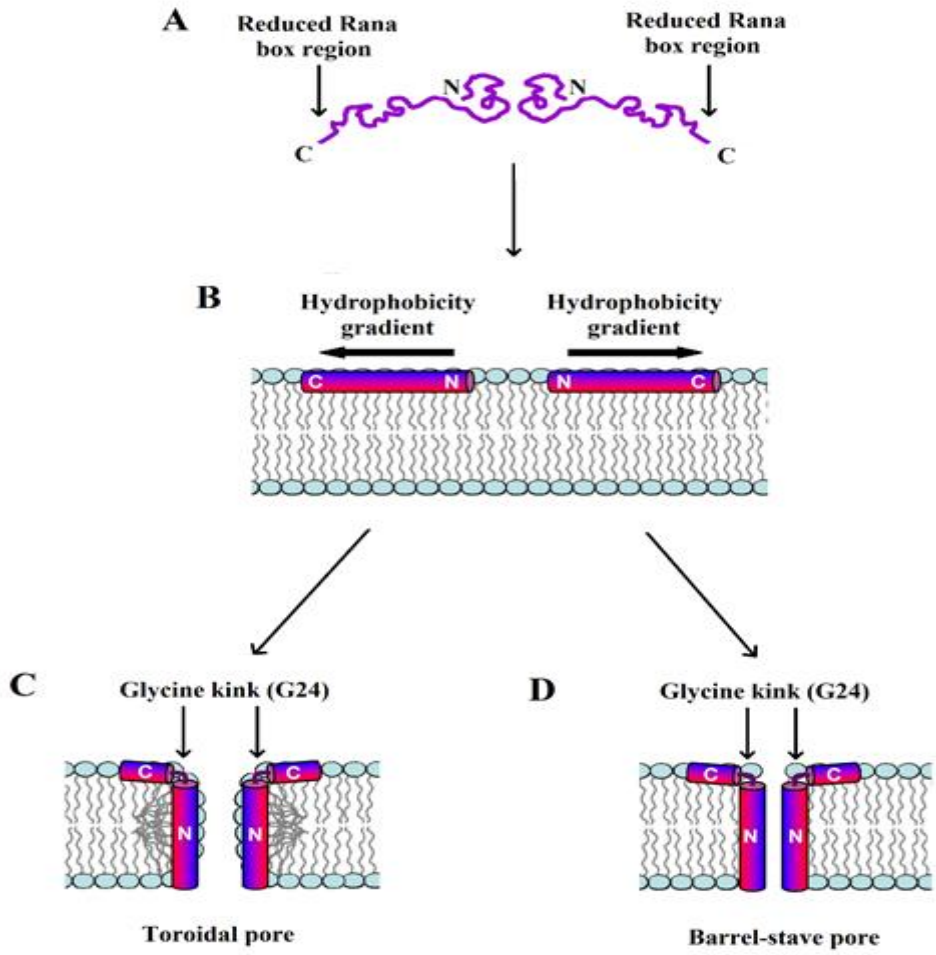

Figure 8 was revised from [19] and shows models for the membrane interaction of E2EM-lin where the peptide is represented as cylinders with a hydrophobic surface (red) and a hydrophilic surface (blue). For clarity, two monomers of E2EM-lin are shown in this pore forming process but it has been predicted that the involvement of higher order oligomers of the peptide are probable [35]. In our model, aqueous E2EM-lin is largely unstructured and targets anionic components of the bacterial cell membrane *via* its strong cationic charge (Figure 8A). Localisation to the membrane interface promotes the adoption of strongly α-helical structure and membrane partitioning by E2EM-lin *via* electrostatic associations with the lipid head-group region and hydrophobic interactions with the acyl chain core (Figure 8B). This action then leads to membrane permeabilisation and ultimately, the death of target bacteria *via* either toroidal pore (Figure 8C) or barrel stave pore formation (Figure 8D). In each case, the N-terminal α-helical structure of the peptide, E2EM-lin (1-23), forms a tilted peptide with an

extensive hydrophobicity gradient that plays a role in promoting the transmembrane orientation of E2EM-lin (Figure 8C and Figure 8D). For the formation of both pore types, a glycine kink (G24) orientates the C-terminal, reduced Rana box region of the peptide, E2EM-lin (25-37) to lie parallel to the membrane surface. In this orientation, the C-terminal region of the peptide interacts with the lipid head-group region of the membrane and stabilises pore formation by E2EM-lin.

In the next stages of our model, partitioning by α-helical E2EM-lin leads to reorientation of the peptide within the bilayer to facilitate membrane lysis (Table 2) and ultimately, the death of the target bacteria (Figure 8); it has previously been proposed that membranolysis by E2EM-lin involves the formation of either toroidal pores (Figure 8C) or barrel stave pores (Figure 8D) [19]. In each case, the α-helical structure adopted by the peptide forms two strongly amphiphilic α-helices defined by the N-terminal residues E2EM-lin (1-23) and the C-terminal residues E2EM-lin (25-37), which are linked by an intervening glycine residue (Figures 1B and 1C). The N-terminal region, E2EM-lin (1-23), exhibits tilted peptide characteristics, with an extensive hydrophobicity gradient, encompassing almost two thirds of its sequence (Figure 2A and Figure 2B). Tilted peptides are known to promote the angled insertion of pore-forming amphibian AMPs into microbial membranes [71] and our model further proposes that similar mechanisms (Figure 7B) may play a role in promoting the transmembrane orientation of the E2EM-lin's N-terminal region (Figure 8C and Figure 8D). This mode of oblique penetration could help explain the observation that insertion by the peptide appears to have a rigidifying effect on the lipid matrix of bacterial membranes, promoting increases in its lipid packing density, which render the membrane thermodynamically unstable (Table 3). It seems possible that the tilted structure possessed by the transmembrane region of E2EM-lin could play a more direct role in pore formation by the peptide; it has been previously shown that these structural motifs are able to promote protein – protein interactions [42]. In relation to the C-terminal region of E2EM-lin, similarly to E2EM, our model proposes that E2EM-lin (24-37) interacts with the membrane surface regions, thereby acting as an anchor that stabilizes pore formation by the peptide (Figures 8C and 8D) [19]. However, in contrast to E2EM, the residues of E2EM-lin (24-37) are not conformationally constrained by the presence of a disulphide bond, which may help promote membrane anchoring by this C-terminal region [25, 33]. Moreover, given the functional redundancy of the disulphide bond in E2EM-lin (24-37), this region may also serve to stabilize the overall α-helical, membrane interactive conformation of E2EM-lin, as proposed for the parent peptide [19, 34, 72]. Indeed, E2EM-lin (24-37) shows the potential to

form tilted structure (Figure 2B) and maintaining the general α-helical conformation of E2EM-lin would stabilize its overall tilted architecture, thereby promoting pore formation [73].

E2EM-lin showed a clear, potent specificity for Gram-positive bacteria that appeared to be promoted by the relative excess of anionic lipid found in their membranes as compared to Gram-negative bacteria (Table 1), although these lipids, PG and CL, appeared to play widely different roles the antibacterial action of the peptide. The levels of PG in membranes of the Gram-positive bacteria studied here were between *circa* one and a half and ten times greater than those of Gram-negative organisms (Table 1). These higher levels of PG induced increased quantities of amphiphilic α-helical structure in E2EM-lin (Table 2), which generally enhanced the ability of the peptide to penetrate and lyse the membranes of *S. aureus* and *B. subtilis* in relation to *E. coli* and *P. aeruginosa* (Table 2, Figure 8B). In terms of our model for the antibacterial activity of E2EM-lin, increased quantities of α-helical structure could contribute to the preference shown by the peptide for Gram-positive *via* a number of structure / function relationships (Figure 8). Clearly, increased amphiphilic α-helical structure would endow E2EM-lin with a greater capacity to engage in the electrostatic and hydrophobic interactions associated with membrane invasion by the peptide. Increased α-helical structure could also potentially, enhance the levels of tilted structure formed by E2EM-lin in its N-terminal region, which was proposed above to help drive the transmembrane orientation of this region. Moreover, the presence of higher levels of α-helical structure in the N-terminal region of E2EM-lin would increase the surface areas of this secondary structure available for the protein – lipid and protein – protein interactions involved in the process of pore formation, thereby increasing the efficacy of this process.

The levels of CL in membranes of the Gram-positive bacteria studied here were four to five times greater than those of Gram-negative organisms, which paralleled a *circa* twentyfold increase in antibacterial potency (Table 1). These observations strongly suggested that CL-mediated mechanisms would make a major contribution to the activity E2EM-lin against *S. aureus* and *B. subtilis*, and the peptide's preference for Gram-positive bacteria. Nonetheless, although CL induced high levels of α-helical structure in E2EM-lin (Table 2), the lipid appeared not to directly promote the membranolytic activity of the peptide. The role of CL in

the antibacterial action of E2EM-lin was unclear but it is well established that the lipid is able to modulate multiple membrane properties that can influence the action of AMPs [74]. This ability underpins a number of antimicrobial mechanisms that have been recently reported for AMPs and has the potential to explain the inability of CL to promote high levels of membranolysis by E2EM-lin [58-60, 75, 76]. In particular, studies on some of these AMPs showed that the high levels of CL found in the membranes of Gram-positive bacteria, such as *S. aureus* (Table 2), were able to inhibit the lytic action of these peptides but not their ability to bind the bilayer surface. This inhibitory action appeared to derive from the intrinsic structural properties of CL; namely the ability of its cone shaped molecule to promote negative membrane curvature, thereby countering the tendency of AMPs to induce positive membrane curvature and inhibiting toroidal pore formation by these peptides [59, 60]. Mechanisms of this type would be consistent with the fact that E2EM-lin interacted with the head-group region of CL membranes but appeared unable to penetrate their hydrophobic acyl chain region (Figure 7A). Presumably, in this paradigm, the major promoter of E2EM-lin activity against Gram-positive bacteria would be PG-driven lytic mechanisms (Figure 7). There is also the possibility that CL promotes the antibacterial activity of E2EM-lin through non-lytic mechanisms of membrane interaction and such mechanisms have recently been reported for a number of AMPs [61, 62]. For example, some AMPs show high activity against *B. subtilis* using a novel mechanism that was based on neither membrane lysis nor the use intracellular sites of action. Rather, this mechanism involved peptide interactions with CL-rich PE microdomains in *B. subtilis* membranes, thereby influencing the functional organization of these membranes and initiating effects on cell metabolism and homeostasis that promoted cell death [61]. Clearly, similar non-membranolytic mechanisms could not feature in the antibacterial action of E2EM-lin against *S. aureus*; PE is absent from the membranes of this organism (Table 2) and in this case, it would seem that the antibacterial action of the peptide would be driven by PG-mediated lytic action (Figure 8). In relation to Gram-negative bacteria, the low PG content of their membranes (Table 2) would suggest that lytic mechanisms driven by this lipid do not make a major contribution to the action of E2EM-lin against these organisms (Figure 8). The low CL content of these membranes (Table 2) also renders it unlikely that mechanisms similar to those described above, which enable the lipid to effectively inhibit the action of AMPs, would have a major impact on the action of E2EM-lin against Gram-negative bacteria [58-60]. PE lipids are by far the major component of membranes from Gram-negative bacteria (Table 2) and non-membranolytic, mechanisms involving interactions with CL-rich PE microdomains have been

reported for AMPs that kill *E. coli* [62]. These mechanisms show similarities to those described above for *B. subtilis* [61] and involve the perturbation of the lipid organization in *E. coli* membranes, which promotes inhibition of the cell division process and death of the organism [62]. It is possible that similar mechanisms may contribute to the action of E2EM-lin against *E. coli* and *P. aeruginosa*; however, based on our data, the primary driving force behind the action of the peptide towards Gram-negative bacteria would seem to be the induction of membranolytic α-helical structure by PE (Figure 4, Table 2). Indeed, the lower ability of this lipid to induce such structure in E2EM-lin (Table 2) in comparison to PG would seem to be a major reason for the peptide's reduced efficacy towards Gram-negative bacteria in relation to Gram-positive bacteria (Table 1). Moreover, similarly to CL, PE is able to modulate multiple membrane properties that can influence the antimicrobial mechanisms of AMPs and in a number of cases, this ability involves the capacity of the cone-shaped molecule possessed by this lipid to promote negative membrane curvature [77]. For example, it was proposed that this ability may help facilitate the preferential extraction of PE from *E. coli* membranes by cycloviolacin O2 from *Viola odorata*, thereby promoting membrane thinning and the membranolytic action of the peptide against this organism [78]. In particular, it is well established that the ability of PE to adopt non-lamellar structures and promote negative membrane curvature enhances the capacity of tilted AMPs to destabilize and permeabilize membranes [79, 80], as proposed for these AMPs when directed against *E. coli* [81]. It seems possible that this ability could help facilitate the action of E2EM-lin against *E. coli*, *P. aeruginosa* and the other Gram-negative organisms studied here, as well as that against some of the Gram-positive bacteria (Table 2).

In conclusion, E2EM-lin shows specificity and potent efficacy towards Gram-positive bacteria, and when taken with the low haemolytic activity of the peptide, the potential for development as an agent to combat these organisms is suggested [35]. Gram-positive bacteria are the causes of many serious clinical infections due to their association with a diverse spectrum of pathologies, particularly those with MDR such as methicillin-resistant *Staphylococcus aureus* and vancomycin-resistant enterococci [82, 83]. This preference for Gram-positive bacteria could also support the suggested role for E2EM-lin as a thermostable, antimicrobial agent in the food industry [35]; a variety of Gram-positive bacteria able to tolerate high temperatures are known to act as food spoilage organisms [84].

Biochimica et Biophysica Acta (BBA) – Biomembranes Volume 1862, Issue 2, 1 February 2020, 183141: https://doi.org/10.1016/j.bbamem.2019.183141

Acknowledgments

This work has been partially funded by Shah Abdul Latif University, Pakistan *via* the Higher Education Commission, Pakistan. The authors are grateful to Stefanie Gilchrist, University of Central Lancashire who aided in supplying the bacteria for the antimicrobial assay.

Author contributions

S.R.D, F.H and D.A.P designed the experiments. E.M, L.H.G.M, S.R.D and K.B performed the experiments. S.R.D, F.H, L.H.G.M and D.A.P wrote the main manuscript text. All authors approved the manuscript.

Conflicts of interest

The authors declare no conflict of interest.

References

[1] B. Aslam, W. Wang, M.I. Arshad, M. Khurshid, S. Muzammil, M.H. Rasool, M.A. Nisar, R.F. Alvi, M.A. Aslam, M.U. Qamar, M.K.F. Salamat, Z. Baloch, Antibiotic resistance: a rundown of a global crisis, Infect Drug Resist, 11 (2018) 1645-1658.

[2] J. Wang, X. Dou, J. Song, Y. Lyu, X. Zhu, L. Xu, W. Li, A. Shan, Antimicrobial peptides: Promising alternatives in the post feeding antibiotic era, Medicinal Research Reviews, 39 (2019) 831-859.

[3] X.Q. Xu, R. Lai, The Chemistry and Biological Activities of Peptides from Amphibian Skin Secretions, Chemical Reviews, 115 (2015) 1760-1846.

[4] J. Patocka, E. Nepovimova, B. Klimova, Q. Wu, K. Kuca, Antimicrobial Peptides: Amphibian Host Defense Peptides, Current medicinal chemistry, (2018).

[5] J. Conlon, A. Sonnevend, Clinical applications of amphibian antimicrobial peptides, Hamdan Medical Journal, 4 (2011) 62-72.

[6] S.R. Dennison, F. Harris, M. Mura, D.A. Phoenix, An atlas of anionic antimicrobial peptides from amphibians, Curr Protein Pept Sci, (2018).

[7] D. Frost, R., Amphibian Species of the World, in: An Online Reference. Version 6.0, American Museum of Natural History, New York, USA., 2019.

[8] E. Konig, O.R. Bininda-Emonds, C. Shaw, The diversity and evolution of anuran skin peptides, Peptides, 63 (2015) 96-117.

[9] J.M. Conlon, Reflections on a systematic nomenclature for antimicrobial peptides from the skins of frogs of the family Ranidae, Peptides, 29 (2008) 1815-1819.

[10] R. Alexander Pyron, J.J. Wiens, A large-scale phylogeny of Amphibia including over 2800 species, and a revised classification of extant frogs, salamanders, and caecilians, Molecular Phylogenetics and Evolution, 61 (2011) 543-583.

[11] D.R. Frost, T. Grant, J. Faivovich, R.H. Bain, A. Haas, C.F.B. Haddad, R.A. De Sa, A. Channing, M. Wilkinson, S.C. Donnellan, C.J. Raxworthy, J.A. Campbell, B.L. Blotto, P. Moler, R.C. Drewes, R.A. Nussbaum, J.D. Lynch, D.M. Green, W.C. Wheeler, The Amphibian Tree of Life., Bull Amer Mus Nat Hist., 297 (2006) 1-370.

[12] Z.-Y. Yuan, W.-W. Zhou, X. Chen, J.N.A. Poyarkov, H.-M. Chen, N.-H. Jang-Liaw, W.-H. Chou, N.J. Matzke, K. Iizuka, M.-S. Min, S.L. Kuzmin, Y.-P. Zhang, D.C. Cannatella, D.M. Hillis, J. Che, Spatiotemporal Diversification of the True Frogs (Genus Rana): A Historical Framework for a Widely Studied Group of Model Organisms, Systematic Biology, 65 (2016) 824-842.

[13] AmphibiaWeb., AmphibiaWeb, in, vol. 2019, University of California., Berkeley, CA, USA., 2019.

[14] P. Thomas, T.V. Kumar, V. Reshmy, K.S. Kumar, S. George, A mini review on the antimicrobial peptides isolated from the genus Hylarana (Amphibia: Anura) with a proposed nomenclature for amphibian skin peptides, Molecular biology reports, 39 (2012) 6943-6947.

[15] J.M. Conlon, A proposed nomenclature for antimicrobial peptides from frogs of the genus Leptodactylus, Peptides, 29 (2008) 1631-1632.

[16] N. Morikawa, K. Hagiwara, T. Nakajima, Brevinin-1 and -2, unique antimicrobial peptides from the skin of the frog, Rana brevipoda porsa, Biochemical and Biophysical Research Communications, 189 (1992) 184-190.

[17] M. Simmaco, G. Mignogna, D. Barra, F. Bossa, Antimicrobial peptides from skin secretions of Rana esculenta. Molecular cloning of cDNAs encoding esculentin and brevinins and isolation of new active peptides, Journal of Biological Chemistry, 269 (1994) 11956-11961.

[18] V.T.V. Kumar, D. Holthausen, J. Jacob, S. George, Host Defense Peptides from Asian Frogs as Potential Clinical Therapies, Antibiotics-Basel, 4 (2015) 136-159.

[19] H.-S. Won, S.-J. Kang, B.-J. Lee, Action mechanism and structural requirements of the antimicrobial peptides, gaegurins, Biochimica et Biophysica Acta (BBA) - Biomembranes, 1788 (2009) 1620-1629.

[20] S.H. Eo, B.-J. Lee, C.-D. Park, J.-H. Jung, N. Hong, W.-S. Lee, Taxonomic identity of the Glandirana emeljanovi (Anura, Ranidae) in Korea revealed by the complete mitochondrial genome sequence analysis, Mitochondrial DNA Part B, 4 (2019) 961-962.

[21] J.M. Park, J.E. Jung, B.J. Lee, Antimicrobial Peptides from the Skin of a Korean Frog, Rana rugosa, Biochemical and Biophysical Research Communications, 205 (1994) 948-954.

[22] S. Kim, S.S. Kim, Y.-J. Bang, S.-J. Kim, B.J. Lee, In vitro activities of native and designed peptide antibiotics against drug sensitive and resistant tumor cell lines, Peptides, 24 (2003) 945-953.

[23] H.S. Won, S.J. Jung, H.E. Kim, M.D. Seo, B.J. Lee, Systematic peptide engineering and structural characterization to search for the shortest antimicrobial peptide analogue of gaegurin 5, J Biol Chem, 279 (2004) 14784-14791.

[24] T.K. Pham, D.H. Kim, B.J. Lee, Y.W. Kim, Truncated and constrained helical analogs of antimicrobial esculentin-2EM, Bioorganic & medicinal chemistry letters, 23 (2013) 6717-6720.

[25] H.S. Won, S.H. Park, H.E. Kim, B. Hyun, M. Kim, B.J. Lee, B.J. Lee, Effects of a tryptophanyl substitution on the structure and antimicrobial activity of C-terminally truncated gaegurin 4, European journal of biochemistry, 269 (2002) 4367-4374.

[26] H.-S. Won, S.-J. Kang, W.-S. Choi, B.-J. Lee, Activity optimization of an undecapeptide analogue derived from a frog-skin antimicrobial peptide, Mol Cells, 31 (2011) 49-54.

[27] S.-W. Chi, J.-S. Kim, D.-H. Kim, S.-H. Lee, Y.-H. Park, K.-H. Han, Solution structure and membrane interaction mode of an antimicrobial peptide gaegurin 4, Biochemical and Biophysical Research Communications, 352 (2007) 592-597.

[28] H.S. Won, M.D. Seo, S.J. Jung, S.J. Lee, S.J. Kang, W.S. Son, H.J. Kim, T.K. Park, S.J. Park, B.J. Lee, Structural determinants for the membrane interaction of novel bioactive undecapeptides derived from gaegurin 5, Journal of medicinal chemistry, 49 (2006) 4886-4895.

[29] S.J. Kang, H.Y. Ji, B.J. Lee, Anticancer activity of undecapeptide analogues derived from antimicrobial peptide, brevinin-1EMa, Arch Pharm Res, 35 (2012) 791-799.

[30] J.H. Kim, J.O. Lee, J.H. Jung, S.K. Lee, G.Y. You, S.H. Park, H.S. Kim, Gaegurin-6 stimulates insulin secretion through calcium influx in pancreatic β Rin5mf cells, Regul. Pept., 159 (2010) 123-128.

[31] S.S. Kim, S. Kim, E. Kim, B. Hyun, K.K. Kim, B.J. Lee, Synergistic Inhibitory Effect of Cationic Peptides and Antimicrobial Agents on the Growth of Oral Streptococci, Caries Research, 37 (2003) 425-430.

[32] I. Bayarbat, J.-H. Lee, S.-Y. Lee, Expression of Recombinant Hybrid Peptide Gaegurin4 and LL37 using Fusion Protein in E. coli, Korean Journal of Microbiology and Biotechnology, 40 (2012) 92-97.

[33] S.H. Park, Y.K. Kim, J.W. Park, B. Lee, B.J. Lee, Solution structure of the antimicrobial peptide gaegurin 4 by 1H and 15N nuclear magnetic resonance spectroscopy, European Journal of Biochemistry, 267 (2000) 2695-2704.

[34] E.F. Haney, H.N. Hunter, K. Matsuzaki, H.J. Vogel, Solution NMR studies of amphibian antimicrobial peptides: Linking structure to function?, Biochimica et Biophysica Acta (BBA) - Biomembranes, 1788 (2009) 1639-1655.

[35] E. Malik, The characterisation of linearized esculentin-2EM (gaegurin 4) at varying pH and in differing lipid environments, in: Forensics and Applied Sciences, vol. PhD, University of Central Lancashire, UK., Preston, UK., 2018, pp. 227.

[36] P.J. Perez Espitia, N. de Fátima Ferreira Soares, J.S. dos Reis Coimbra, N.J. de Andrade, R. Souza Cruz, E.A. Alves Medeiros, Bioactive Peptides: Synthesis, Properties, and Applications in the Packaging and Preservation of Food, Comprehensive Reviews in Food Science and Food Safety, 11 (2012) 187-204.

[37] E.M. Del Aguila, L.P. Gomes, C.S. Freitas, P.R. Pereira, V.F. Paschoalin, Natural Antimicrobials in Food Processing: Bacteriocins, Peptides and Chitooligosaccharides, in: Atta-ur-Rahman., M.I. Choudhary (Eds.) Frontiers in Anti-Infective Drug Discovery, vol. 5, Bentham Sciences., 2017, pp. 55-108.

[38] R. Gautier, D. Douguet, B. Antonny, G. Drin, HELIQUEST: a web server to screen sequences with specific alpha-helical properties, Bioinformatics, 24 (2008) 2101-2102.

[39] D.A. Phoenix, F. Harris, The hydrophobic moment and its use in the classification of amphiphilic structures (Review), Molecular Membrane Biology, 19 (2002) 1-10.

[40] F. Harris, J. Wallace, D.A. Phoenix, Use of hydrophobic moment plot methodology to aid the identification of oblique orientated alpha-helices, Mol Membr Biol, 17 (2000) 201-207.

[41] D.A. Phoenix, S.R. Dennison, F. Harris, Models for the Membrane Interactions of Antimicrobial Peptides, in: Antimicrobial Peptides, Wiley-VCH Verlag GmbH & Co. KGaA, 2013, pp. 145-180.

[42] F. Harris, A. Daman, J. Wallace, S.R. Dennison, D.A. Phoenix, Oblique orientated alpha-helices and their prediction, Current Protein & Peptide Science, 7 (2006) 529-537.
[43] E.G. Bligh, W.J. Dyer, A rapid method of total lipid extraction and purification, Canadian journal of biochemistry and physiology, 37 (1959) 911-917.
[44] N.J. Greenfield, Using circular dichroism spectra to estimate protein secondary structure, Nature protocols, 1 (2006) 2876-2890.
[45] L. Whitmore, B. Woollett, A.J. Miles, R.W. Janes, B.A. Wallace, The protein circular dichroism data bank, a Web-based site for access to circular dichroism spectroscopic data, Structure, 18 (2010) 1267-1269.
[46] L. Whitmore, B.A. Wallace, Protein secondary structure analyses from circular dichroism spectroscopy: methods and reference databases, Biopolymers, 89 (2008) 392-400.
[47] L. Whitmore, B.A. Wallace, DICHROWEB, an online server for protein secondary structure analyses from circular dichroism spectroscopic data, Nucleic Acids Res, 32 (2004) W668-673.
[48] S.R. Dennison, S. Dante, T. Hauß, K. Brandenburg, F. Harris, D.A. Phoenix, Investigations into the membrane interactions of m-calpain domain V, Biophysical journal, 88 (2005) 3008-3017.
[49] S.R. Dennison, F. Harris, M. Mura, L.H.G. Morton, A. Zvelindovsky, D.A. Phoenix, A Novel Form of Bacterial Resistance to the Action of Eukaryotic Host Defense Peptides, the Use of a Lipid Receptor, Biochemistry, 52 (2013) 6021-6029.
[50] S.R. Dennison, F. Harris, D.A. Phoenix, A Langmuir Approach Using Monolayer Interactions to Investigate Surface Active Peptides, Protein and Peptide Letters, 17 (2010) 1363-1375.
[51] J.T. Davies, E.K. Rideal, Interfacial Phenomena, 2nd ed., Academic Press, New York, 1963.
[52] J. Todd, Introduction to the Constructive Theory of Functions, Academic Press, New York, 1963.
[53] S.-H. Park, Y.-K. Kim, J.-W. Park, B. Lee, B.-J. Lee, Solution structure of the antimicrobial peptide gaegurin 4 by 1H and 15N nuclear magnetic resonance spectroscopy, 267 (2000) 2695-2704.
[54] M. El Khoury, J. Swain, G. Sautrey, L. Zimmermann, P. Van Der Smissen, J.-L. Décout, M.-P. Mingeot-Leclercq, Targeting Bacterial Cardiolipin Enriched Microdomains: An

Antimicrobial Strategy Used by Amphiphilic Aminoglycoside Antibiotics, Scientific reports, 7 (2017) 10697-10697.

[55] J. Swain, M. El Khoury, J. Kempf, F. Briée, P. Van Der Smissen, J.-L. Décout, M.-P. Mingeot-Leclercq, Effect of cardiolipin on the antimicrobial activity of a new amphiphilic aminoglycoside derivative on Pseudomonas aeruginosa, PloS one, 13 (2018) e0201752-e0201752.

[56] G. Sautrey, M. El Khoury, A.G. Dos Santos, L. Zimmermann, M. Deleu, L. Lins, J.L. Decout, M.P. Mingeot-Leclercq, Negatively Charged Lipids as a Potential Target for New Amphiphilic Aminoglycoside Antibiotics: A BIOPHYSICAL STUDY, J Biol Chem, 291 (2016) 13864-13874.

[57] C.W. Johnston, M.A. Skinnider, C.A. Dejong, P.N. Rees, G.M. Chen, C.G. Walker, S. French, E.D. Brown, J. Bérdy, D.Y. Liu, N.A. Magarvey, Assembly and clustering of natural antibiotics guides target identification, Nature Chemical Biology, 12 (2016) 233.

[58] T.H. Zhang, J.K. Muraih, N. Tishbi, J. Herskowitz, R.L. Victor, J. Silverman, S. Uwumarenogie, S.D. Taylor, M. Palmer, E. Mintzer, Cardiolipin Prevents Membrane Translocation and Permeabilization by Daptomycin, Journal of Biological Chemistry, 289 (2014) 11584-11591.

[59] L. Hernández-Villa, M. Manrique-Moreno, C. Leidy, M. Jemioła-Rzemińska, C. Ortíz, K. Strzałka, Biophysical evaluation of cardiolipin content as a regulator of the membrane lytic effect of antimicrobial peptides, Biophysical Chemistry, 238 (2018) 8-15.

[60] D. Poger, S. Poyry, A.E. Mark, Could Cardiolipin Protect Membranes against the Action of Certain Antimicrobial Peptides? Aurein 1.2, a Case Study, ACS omega, 3 (2018) 16453-16464.

[61] K. Scheinpflug, O. Krylova, H. Nikolenko, C. Thurm, M. Dathe, Evidence for a Novel Mechanism of Antimicrobial Action of a Cyclic R-,W-Rich Hexapeptide, Plos One, 10 (2015).

[62] D. Zweytick, B. Japelj, E. Mileykovskaya, M. Zorko, W. Dowhan, S.E. Blondelle, S. Riedl, R. Jerala, K. Lohner, N-acylated peptides derived from human lactoferricin perturb organization of cardiolipin and phosphatidylethanolamine in cell membranes and induce defects in Escherichia coli cell division, PLoS One, 9 (2014) e90228.

[63] C. Ratledge, S.G. Wilkinson, Microbial lipids, Academic Press London, 1988.

[64] K. Lohner, E.J. Prenner, Differential scanning calorimetry and X-ray diffraction studies of the specificity of the interaction of antimicrobial peptides with membrane-mimetic systems, Biochimica et Biophysica Acta (BBA) - Biomembranes, 1462 (1999) 141-156.

[65] S.R. Dennison, L.H. Morton, F. Harris, D.A. Phoenix, Low pH Enhances the Action of Maximin H5 against Staphylococcus aureus and Helps Mediate Lysylated Phosphatidylglycerol-Induced Resistance, Biochemistry, 55 (2016) 3735-3751.

[66] S.R. Dennison, L.H.G. Morton, K. Brandenburg, F. Harris, D.A. Phoenix, Investigations into the ability of an oblique alpha-helical template to provide the basis for design of an antimicrobial anionic amphiphilic peptide, Febs Journal, 273 (2006) 3792-3803.

[67] F. Harris, S.R. Dennison, D.A. Phoenix, Aberrant action of amyloidogenic host defense peptides: a new paradigm to investigate neurodegenerative disorders?, Faseb J, 26 (2012) 1776-1781.

[68] V.T. Kumar, D. Holthausen, J. Jacob, S. George, Host defense peptides from Asian frogs as potential clinical therapies, Antibiotics, 4 (2015) 136-159.

[69] P. Abraham, A. Sundaram, A. R, R. V, S. George, K.S. Kumar, Structure-Activity Relationship and Mode of Action of a Frog Secreted Antibacterial Peptide B1CTcu5 Using Synthetically and Modularly Modified or Deleted (SMMD) Peptides, PLoS One, 10 (2015) e0124210.

[70] E. Malik, S.R. Dennison, F. Harris, D.A. Phoenix, Eukaryotic antimicrobial peptides with pH dependent mechanisms of action, Pharmaceuticals, In press (2016).

[71] M. Mura, S.R. Dennison, A.V. Zvelindovsky, D.A. Phoenix, Aurein 2.3 functionality is supported by oblique orientated alpha-helical formation, Biochim Biophys Acta, 1828 (2013) 586-594.

[72] H. Kim, S. Kim, M. Lee, B. Lee, P. Ryu, Role of C- terminal heptapeptide in pore-forming activity of antimicrobial agent, gaegurin 4, The Journal of peptide research, 64 (2004) 151-158.

[73] L. Lins, R. Brasseur, Tilted peptides: a structural motif involved in protein membrane insertion?, J Pept Sci, 14 (2008) 416-422.

[74] R.N. Lewis, R.N. McElhaney, The physicochemical properties of cardiolipin bilayers and cardiolipin-containing lipid membranes, Biochimica et Biophysica Acta (BBA)-Biomembranes, 1788 (2009) 2069-2079.

[75] K. Matsuzaki, K. Sugishita, N. Ishibe, M. Ueha, S. Nakata, K. Miyajima, R.M. Epand, Relationship of membrane curvature to the formation of pores by magainin 2, Biochemistry, 37 (1998) 11856-11863.

[76] M.P. dos Santos Cabrera, S.T.B. Costa, B.M. de Souza, M.S. Palma, J.R. Ruggiero, J.J.E.B.J. Ruggiero Neto, Selectivity in the mechanism of action of antimicrobial mastoparan peptide Polybia-MP1, 37 (2008) 879.

[77] D.A. Phoenix, F. Harris, M. Mura, S.R. Dennison, The increasing role of phosphatidylethanolamine as a lipid receptor in the action of host defence peptides, Progress in lipid research, 59 (2015) 26-37.

[78] R. Burman, A.A. Strömstedt, M. Malmsten, U. Göransson, Cyclotide–membrane interactions: Defining factors of membrane binding, depletion and disruption, Biochimica et Biophysica Acta (BBA) - Biomembranes, 1808 (2011) 2665-2673.

[79] B. Bechinger, K. Lohner, Detergent-like actions of linear amphipathic cationic antimicrobial peptides, Biochimica et Biophysica Acta (BBA) - Biomembranes, 1758 (2006) 1529-1539.

[80] A. Thomas, R. Brasseur, Tilted peptides: The history, Current Protein and Peptide Science, 7 (2006) 523-527.

[81] S.R. Dennison, L.H.G. Morton, F. Harris, D.A. Phoenix, The impact of membrane lipid composition on antimicrobial function of an alpha-helical peptide, Chemistry and Physics of Lipids, 151 (2008) 92-102.

[82] N. Woodford, D.M. Livermore, Infections caused by Gram-positive bacteria: a review of the global challenge, Journal of Infection, 59 (2009) S4-S16.

[83] F. Menichetti, Current and emerging serious Gram-positive infections, Clinical Microbiology and Infection, 11 (2005) 22-28.

[84] S. Rawat, Food Spoilage: Microorganisms and their prevention, Asian Journal of Plant Science and Research., 5 (2015) 47-56.

Biochimica et Biophysica Acta (BBA) – Biomembranes Volume 1862, Issue 2, 1 February 2020, 183141: https://doi.org/10.1016/j.bbamem.2019.183141

Biochimica et Biophysica Acta (BBA) – Biomembranes Volume 1862, Issue 2, 1 February 2020, 183141: https://doi.org/10.1016/j.bbamem.2019.183141

Supplementary data

Figure 1. Mass spectrometry data for E2EM-lin

A. E2EM GILDTLKQFAKGVGKDLVKGAAQGVLSTVSC*KLAKTC*

Chemical Formula: $C_{165}H_{285}N_{45}O_{49}S_2$
Exact Mass: 3745.06
Molecular Weight: 3747.48
m/z: 3746.07 (100.0%), 3747.07 (95.9%), 3748.07 (78.3%), 3745.06 (56.0%), 3749.07 (25.7%), 3749.08 (22.2%), 3747.06 (21.8%), 3750.08 (11.4%), 3748.06 (11.0%), 3746.06 (10.2%), 3750.07 (8.5%), 3751.07 (3.5%), 3749.06 (2.1%), 3750.06 (1.5%)
Elemental Analysis: C, 52.88; H, 7.67; N, 16.82; O, 20.92; S, 1.71

B. E2EM-lin GILDTLKQFAKGVGKDLVKGAAQGVLSTVSCKLAKTC

Chemical Formula: $C_{165}H_{287}N_{45}O_{49}S_2$
Exact Mass: 3747.08
Molecular Weight: 3749.50
m/z: 3748.08 (100.0%), 3749.09 (80.5%), 3750.09 (57.7%), 3747.08 (50.8%), 3751.09 (36.1%), 3750.08 (22.6%), 3749.08 (21.8%), 3751.08 (9.3%), 3752.09 (7.0%), 3752.08 (6.3%), 3752.10 (6.0%), 3749.07 (4.6%), 3753.09 (2.6%), 3754.09 (1.1%)
Elemental Analysis: C, 52.86; H, 7.72; N, 16.81; O, 20.91; S, 1.71

C. Mass spectrum of E2EM-lin

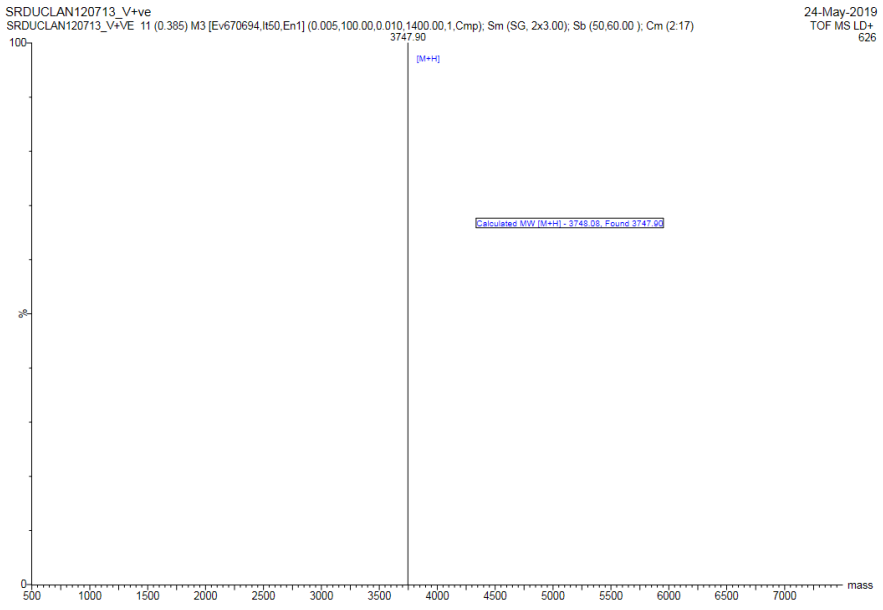

Figure 1C shows a MALDI-TOF time-of-flight mass spectrum of positive ions from E2EM-lin at a mass of 3747.67, confirming the prediction of Chemdraw (Figures 1A and 1B).

Biochimica et Biophysica Acta (BBA) – Biomembranes Volume 1862, Issue 2, 1 February 2020, 183141: https://doi.org/10.1016/j.bbamem.2019.183141

Figure 2. The analysis of E2EM-lin in aqueous solution and organic solvents.

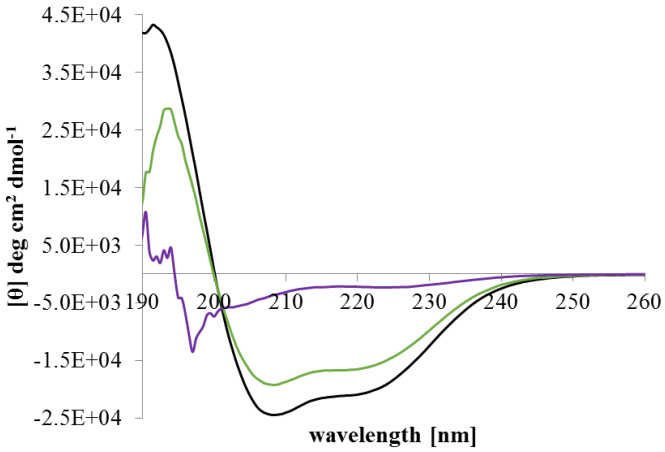

Figure 2 shows CD spectra of E2EM-lin in different environmental conditions. In aqueous solution (PBS, 10.0 mM, pH 7.4), the peptide displayed spectra with a minimum at 200 nm and a weak band near 222 nm (Purple curve), which indicated random coil and β-type structures. In contrast, in individual TFE (Black curve) and a 50 % (v/v) mixture of TFE / PBS (10.0 mM, pH 7.4), E2EM-lin displayed curves with two minima near 210 and 224 nm, respectively, and maxima at 193 nm (Green curve), which is typical of α-helical peptides [44]. Analysis of these spectra showed that E2EM-lin exhibited levels of α-helicity that were 9.3% in aqueous solution (PBS, 10.0 mM, pH 7.4), 66.0% in TFE and 72.0% in 50 % (v/v) mixture of TFE / PBS (10.0 mM, pH 7.4). In each case, the remaining structural contributions were from random coil and β-type structures.

Biochimica et Biophysica Acta (BBA) – Biomembranes Volume 1862, Issue 2, 1 February 2020, 183141: https://doi.org/10.1016/j.bbamem.2019.183141

Figure 3. Pressure–area isotherms for E2EM-lin / lipid monolayers

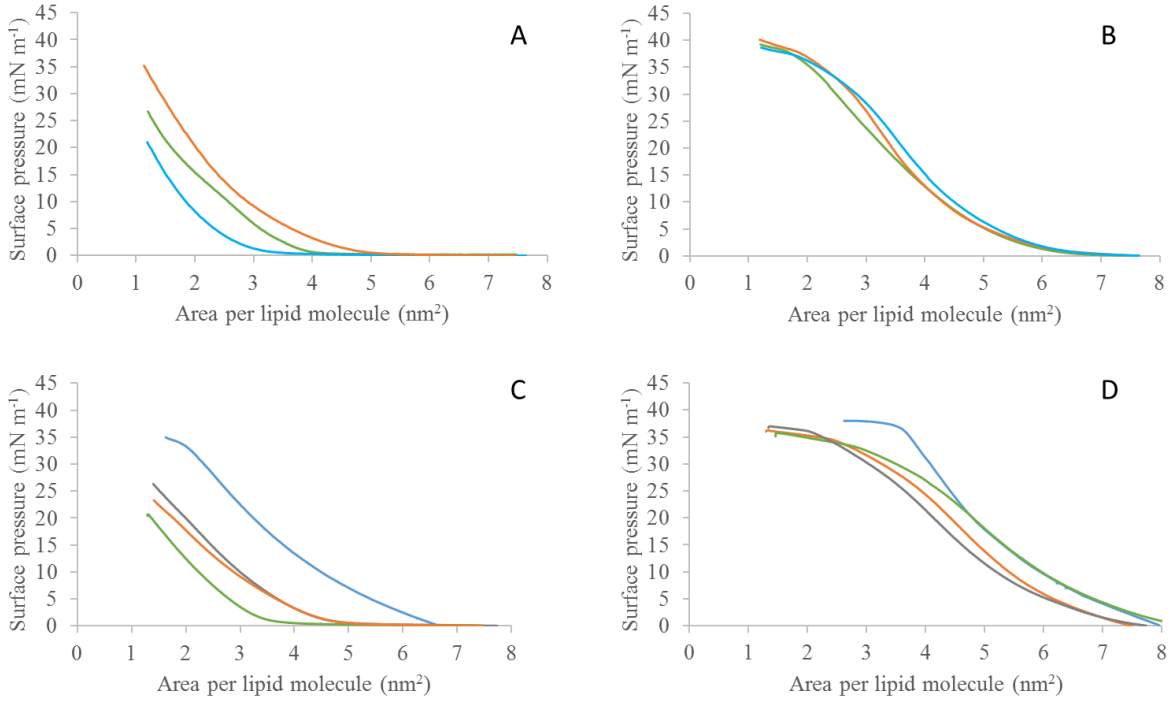

Figure 3 shows pressure–area isotherms for lipid monolayers in the absence and presence of E2EM-lin. Figures 3A and 3B show isotherms for DMPG (Orange), CL (Green) and DMPE (Turquoise) in the absence and presence of E2EM-lin, respectively. Figures 3C and 3D show isotherms for lipid monolayer mimics of bacterial membranes from *E. coli* (Blue), *P. aeruginosa* (Green), *B. subtilis* (Grey) and *S. aureus* (Orange) in the absence and presence of E2EM-lin, respectively. In all cases, in the absence of peptide, these lipid monolayers showed collapse pressures that ranged between 20.0 mN m^{-1} and 35.0 mN m^{-1} (Figure 3A and 3C) but in the presence of E2EM-lin, collapse pressures varied between 35.0 mN m^{-1} and 40.0 mN m^{-1} (Figures 3B and 3D). Analysis of these isotherms showed that for each of the bacterial membranes studied, the presence of the peptide led to increases in C_s^{-1} and values of $\Delta G_{mix} > 0$ (Table 3), consistent with partitioning by E2EM-lin and thermodynamic destabilisation of the these membranes [50]. In each case, the data are the mean of five replicates.